Molecular Imaging
Volume 17: 1-10
© The Author(s) 2018
Article reuse guidelines:
sagepub.com/journals-permissions
DOI: 10.1177/1536012118801223
journals.sagepub.com/home/mix
SAGE

Application of Immuno-PET in Antibody–Drug Conjugate Development

Kendra S. Carmon, PhD[1] and Ali Azhdarinia, PhD[1]

Abstract

Targeted therapies hold great promise for cancer treatment and may exhibit even greater efficacy when combined with patient selection tools. The clinical impact of identifying likely responders includes reducing the number of unnecessary and ineffective therapies as well as more accurately determining drug effects. Positron emission tomography (PET) imaging using zirconium-89 radiolabeled monoclonal antibodies (mAbs), also referred to as zirconium-89 (^{89}Zr)-immuno-PET, provides a potential biomarker to measure target expression and verify optimal delivery of targeted agents to tumors. Antibody–drug conjugates (ADCs) combine the high affinity and specificity of mAbs with the potency of cytotoxic drugs to target tumor-expressing antigen and destroy cancer cells. Thus, ^{89}Zr-immuno-PET of whole-body biodistribution, pharmacokinetics, and tumor targeting of antibodies and ADCs to predict toxicity and efficacy could help guide individualized treatment. Here, we review how ^{89}Zr-immuno-PET is being used as a companion diagnostic with the development of ADCs. Furthermore, we discuss how ^{89}Zr-immuno-PET may be utilized in future clinical trials as an adjunct tool with novel ADCs to select cancer patients who have the greatest potential to benefit from treatment and improve ADC dosing regimens.

Keywords

immuno-PET, antibody–drug conjugates, cancer, molecular imaging, companion diagnostics

Antibody–Drug Conjugates

An Emerging Class of Cancer Therapeutics

Antibody–drug conjugates (ADCs), also referred to as guided missiles or targeted warheads, are one of the fastest growing classes of cancer therapeutics. Over the past decade, several advances have been made to identify novel targets and improve ADC stability and efficacy. Generation of a successful ADC depends on four main components: the target antigen, antibody, linker, and cytotoxic payload (Figure 1).[1] These immunoconjugates utilize highly specific monoclonal antibodies (mAbs) to deliver extremely potent cytotoxins (ie, subnanomolar half maximal inhibitory concentration values) to the tumor site through antigen targets that are enriched on the cancer cell surface.[2,3] A covalent linker couples the cytotoxin to the mAb, providing stability and safety during systemic circulation by conferring a therapeutic index to the cytotoxin and limiting off-target effects.[3]

To date, there are four ADCs that have gained regulatory approval by the US Food and Drug Association (FDA) for cancer treatment. Gemtuzumab ozogamicin developed by Wyeth was the first ADC approved in 2000 for the treatment of $CD33^+$ acute myeloid leukemia.[4] However, it was voluntarily withdrawn from the market in 2010 due to dose-related toxicity but, after a postapproval study, was reintroduced into the market by Pfizer in 2017. In 2011, brentuximab vedotin (Adcentis, Seattle Genetics), which targets CD30, was approved for the treatment of anaplastic large cell lymphoma (ALCL) and Hodgkin lymphoma,[5] followed by approval of trastuzumab emtansine (T-DM1, Roche) in 2013 for the treatment of human epidermal growth factor receptor 2 $(HER2)^+$ metastatic breast cancer[6] and inotuzumab ozogamicin (Pfizer) for the treatment of $CD22^+$ relapsed or refractory B-cell precursor acute lymphoblastic leukemia in 2017.[7] There are currently more than 60 ADCs in clinical trials and several more at the preclinical stage for the treatment of hematological malignancies and solid tumors.[8,9]

[1] Institute of Molecular Medicine, McGovern Medical School, The University of Texas Health Science Center at Houston, Houston, TX, USA

Submitted: 10/05/2018. Revised: 01/08/2018. Accepted: 01/08/2018.

Corresponding Authors:
Kendra S. Carmon and Ali Azhdarinia, Institute of Molecular Medicine, McGovern Medical School, The University of Texas Health Science Center at Houston, 1825 Pressler Street, SRB, Houston, TX77030, USA.
Emails: kendra.s.carmon@uth.tmc.edu; ali.azhdarinia@uth.tmc.edu

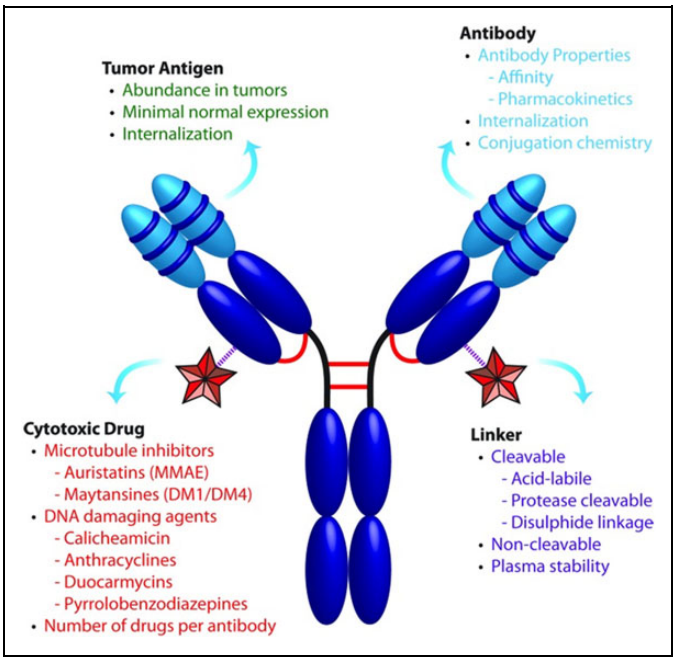

Figure 1. Critical components that influence ADC therapeutics. ADCs consist of a cytotoxic drug conjugated to a mAb via a select linker at choice attachment sites. These components all affect ADC efficacy and safety, and their optimization is essential for successful development (adapted from Panowski et al).[1]

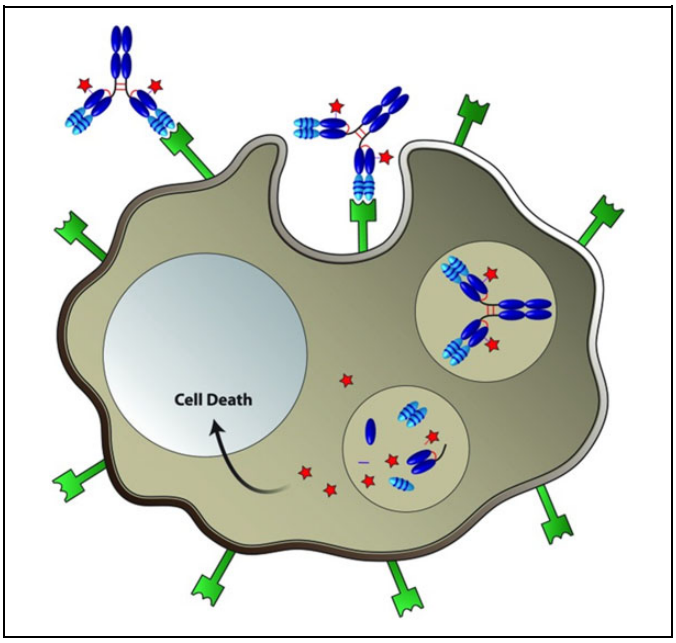

Figure 2. Targeted delivery of cytotoxic drugs to cancer cells by ADCs. The ADC selectively binds a cell-surface tumor antigen, resulting in internalization of the ADC–antigen complex via endocytosis. The ADC–antigen complex then traffics to lysosomal compartments and is degraded to release active cytotoxic drug inside the cell, resulting in cancer cell death (adapted from Panowski et al).[1]

Target Antigen and Antibody Selection

An important consideration in the development of successful ADCs for cancer treatment is the identification of valid antigens for mAb generation and therapeutic targeting. Acceptable antigens must have (1) high expression in tumors with minimal to no expression in normal tissues, (2) localized expression on the tumor cell surface for accessibility to circulating mAbs, and (3) the ability to undergo internalization for transport into the tumor cell followed by intracellular trafficking for processing and payload release[3] (Figure 2). Among the different target antigens being evaluated in preclinical and clinical trials, a number of them are directed against a specific solid tumor type such as carcinoembryonic antigen-related cell adhesion molecule 5 for metastatic colon cancer,[10] whereas others are directed against several tumor types (eg, mesothelin [MSLN] and delta-like 3)[11-13] or against blood cancers (eg, CD37).[14] ADCs are also being developed to target tumor microenvironment proteins such as transmembrane 4 L6 family member 1[15] and cancer stem cell targets including leucine-rich repeat-containing G protein-coupled receptor 5 (LGR5).[16,17] Interestingly, ADC technology is also being evaluated for nononcologic indications including the delivery of antibiotics conjugated to an anti-*Staphylococcus aureus* mAb to treat infection,[18] and the delivery of the tyrosine kinase inhibitor dasatinib to T lymphocytes via a chemokine receptor type 4-targeted mAb to repress T cell activation.[19]

The antibody selected for ADC development is a major determinant of efficacy and toxicity in vivo. In order to maximize the therapeutic index of an ADC, the antibody must have high specificity for the target antigen while exhibiting low uptake in normal tissues or cross-reactivity with other nonspecific antigens that can result in toxicity or faster rate of clearance.[20,21] The minimum threshold of expression that makes a tumor antigen an effective ADC target varies depending on its unique components, including rate and extent of internalization, turnover, and accessibility. Threshold expression levels that have been reported include p97 (10, 000-280, 000 copies/cell, anti-p97-auristatin), prostate-specific membrane antigen (PSMA) (10 000-100 000 copies/cell, anti-PSMA-auristatin), and CD33 (5000-10 000 copies/cell, gemtuzumab ozogamicin).[22-24] However, an endothelin B receptor-targeting ADC was shown to affect xenograft tumor growth with only 1500 copies/cell,[25] whereas other ADC targets such as HER2 have much higher copy numbers ($\sim 10^6$ copies/cell).[26] The antibody must also have high affinity (picomolar range) to ensure sufficient tumor uptake and payload delivery, pharmacokinetic properties that balance drug delivery to tumors and minimize drug exposure to nontarget tissues, and low immunogenicity. It is important to note that while the antibody selected for ADC development may exhibit therapeutic activity prior to payload conjugation, it is not essential.[16]Given the importance of these attributes in predicting the success of ADC therapies, methods to assess targeting, biodistribution, and pharmacokinetics have emerged as an important part in the drug development process.

Table 1. Radionuclides Typically Used for Immuno-PET.

Radionuclide	Half-Life	Max β^+ Energy, MeV
^{64}Cu	12.7 hours	0.66
^{86}Y	14.7 hours	1.2
^{89}Zr	3.3 dys	0.90
^{124}I	4.2 days	2.15

Abbreviations: ^{64}Cu, copper-64; ^{86}Y, yttrium-86; ^{89}Zr, zirconium-89, ^{124}I, iodine-124.

Companion Diagnostics in ADC Development

Applications of Immuno-PET

A key step in the development of new stand-alone cancer therapies is to show compelling preclinical evidence for improved antitumor efficacy with limited toxicity. One approach to address these issues is by employing companion diagnostics that can be used to visually monitor and track therapeutics in vivo.[27] Companion diagnostics are tools or assays that can identify the presence or absence of a biomarker and, when used for molecular imaging, may be useful for predicting therapeutic response. Imaging of radiolabeled mAbs by positron emission tomography (PET), or immuno-PET, has been employed for the noninvasive quantification of mAb uptake in normal and tumor tissues for drug development purposes[28-30] and expanded to ADC development.[31-33] Unlike the assessment of tumor biopsies, which represent characteristics of a specific tumor section, radiolabeling the naked mAb used in an ADC permits global assessment of antigen expression and identification of patients who are likely to respond to a particular ADC therapy. Moreover, tumor heterogeneity between, as well as within, patients can be more effectively understood through comprehensive in vivo assessment of tumors by immuno-PET. A companion diagnostic could also help predict treatment effects, and potentially outcomes, of ADC therapy based on quantitative characterization of tracer uptake, pharmacokinetics, and clearance. Optimally, the biodistribution of the companion diagnostic and the corresponding ADC would be equivalent. The findings could then be used for dose optimization to enhance the safety profile of the ADC in patients in order to maximize antitumor effects. Furthermore, clinical questions related to treatment efficacy could be addressed through the use of a companion diagnostic that accurately measures antigen expression, especially in metastases where the antigen expression profile may not reflect that of the primary tumor.

Radiolabeled Agents for Immuno-PET

The exceptional target specificity of antibodies has led to their use as targeting vehicles for delivery of payloads such as radionuclides for imaging and therapy, fluorescent dyes for intraoperative imaging, and cytotoxic compounds for targeted drug delivery. For immuno-PET agents, different radiolabels (Table 1) can be introduced through a variety of approaches that have been extensively reviewed elsewhere.[34-37] In this review, we focus on the use of the positron-emitting radiometal, zirconium-89 (^{89}Zr), based on its emergence as the radionuclide of choice for antibody imaging and a large number of clinical trials employing ^{89}Zr-immuno-PET.[27,38,39] The increasing adoption of ^{89}Zr for antibody labeling is due in part to its 3.3 day half-life that enables delayed imaging at time points (up to 7 days postinjection) that allow tracer clearance and improved tumor visualization. Although ^{124}I has a longer half-life compared to ^{89}Zr (Table 1), it is not residualizing and therefore is not compatible with an mAb that undergoes internalization.[29] On the other hand, the short half-lives of ^{64}Cu and ^{86}Y can fail to accurately predict mAb biodistribution. The half-life of ^{89}Zr also allows shipping to regional and distant sites, making it possible for researchers and clinicians without access to a cyclotron facility to obtain ^{89}Zr for preclinical or clinical research.

Well-defined manufacturing processes have further contributed to the growing use of ^{89}Zr in molecular imaging. The bifunctional chelator, desferrioxamine (DFO), forms a coordination complex with ^{89}Zr that is efficiently produced and stable (Figure 3).[40-42] Importantly, methods for DFO conjugation have been optimized to produce chelator–protein ratios that retain immunoreactivity and provide sufficient specific activity preparations for microdosing.[43,44] This helped establish good manufacturing practices for ^{89}Zr-labeled mAbs and harmonization of quantitative ^{89}Zr-immuno-PET imaging to support the expanded evaluation of agents in multicenter trials.[38] Since immuno-PET can determine target expression and uptake at the tumor site and at the whole-body level, it can provide a noninvasive method to accurately predict the biodistribution and pharmacokinetics of ADCs in development, which has been typically lacking from phase I studies. Below, we present preclinical and clinical studies that employ^{89}Zr-immuno-PET with the aim of improving treatment outcomes with ADC therapy.

Immuno-PET in Preclinical Evaluation of ADCs

CD30 in Lymphoma

CD30 is a member of the tumor necrosis factor receptor superfamily and is expressed in several cancers including Hodgkin lymphoma, T-cell lymphomas, and large B-cell lymphoma.[45] Since CD30 expression is found only in activated T and B cells, it has been exploited as a target for ADC therapy. Conjugation of monomethyl auristatin E (MMAE) to an anti-CD30 mAb led to the development of the FDA-approved ADC, brentuximab vedotin, for treatment of patients with relapsed or refractory CD30$^+$ Hodgkin lymphoma and ALCL. Currently, brentuximab vedotin is being tested in more than 70 clinical trials to determine its effectiveness as an earlier line of therapy and potential application in additional types of CD30$^-$ expressing lymphomas.[46] Histological assessment of CD30 is the gold

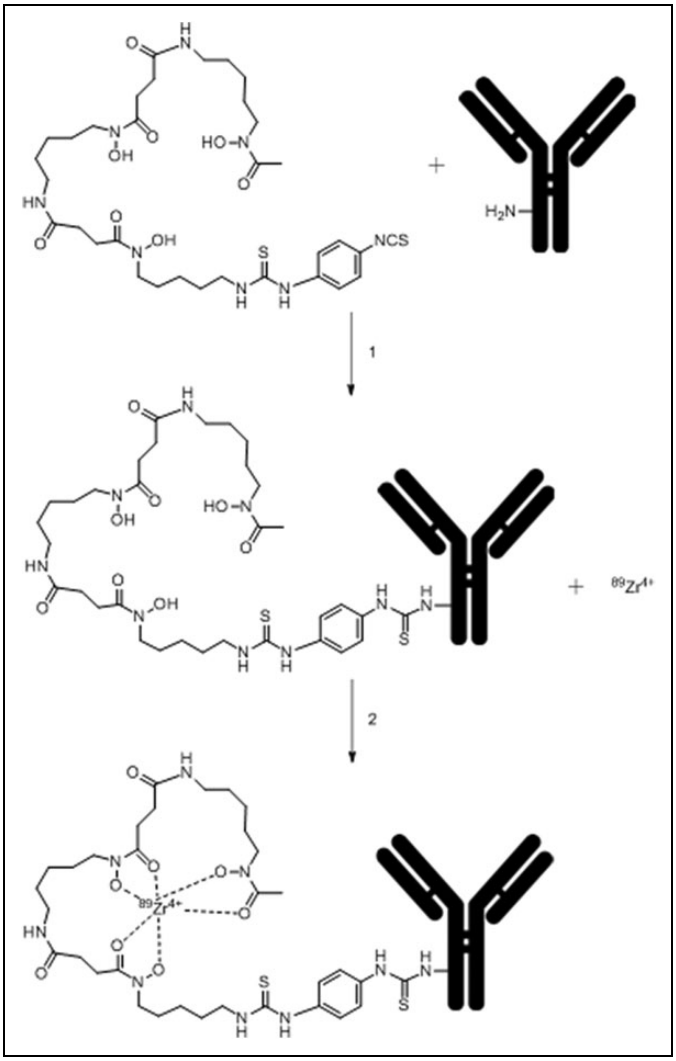

Figure 3. Schematic representation of antibody conjugation with amine-reactive DFO (1) and radiolabeling with ^{89}Zr (2).

standard for determining expression; however, results from multiple studies showing clinical response to brentuximab vedotin in patients who were histologically negative for CD30 demonstrate the need for alternative receptor detection methods. In order to more accurately assess CD30 expression, Rylova and colleagues labeled the anti-CD30 mAb, known as AC-10, with ^{89}Zr to examine its potential as a companion diagnostic for patient selection, prediction of response, and treatment monitoring.[47] In vitro characterization of ^{89}Zr-DFO-AC-10 revealed >98% specific binding in cells that were CD30$^+$, whereas CD30$^-$ cells did not have specific uptake. PET and biodistribution data also showed CD30$^-$ mediated uptake with a peak value of 37.9% $\pm$ 8.2% injected dose/gram (%ID/g) in the CD30$^+$ model 72 hours postinjection, while CD30$^-$ mice had 11.0%ID/g $\pm$ 0.4%ID/g. Target specificity was further confirmed by in vivo blocking experiments, which resulted in a 40% reduction in tumor uptake in CD30$^+$ mice. Immuno-PET showed clear differences between tracer uptake and image contrast in CD30$^+$ and CD30$^-$ groups up to 144 hours postinjection and correlated with autoradiography results from tumor sections (Figure 4). From these findings, the authors demonstrated that ^{89}Zr-DFO-AC-10 may be useful for noninvasive assessment of CD30 status and could potentially serve as companion diagnostic for brentuximab vedotin therapy.

MSLN in Pancreatic and Ovarian Cancer

MSLN is a membrane-bound surface glycoprotein with relatively unknown function yet is highly expressed in mesotheliomas and in pancreatic and ovarian tumors with minimal expression in normal tissues. Studies evaluating anti-MSLN ADCs have shown some promise for the treatment of MSLN-expressing tumors, including maytansinoid DM4-conjugated BAY 94-9343 (Bayer) in a phase II trial and BMS-986148 conjugated with an undisclosed payload which is in a phase I/IIa trial.[8] In 2015, a clinical study was performed to evaluate another anti-MSLN antibody (MMOT05530A) using ^{89}Zr-immuno-PET imaging in conjunction with a phase I trial with the MMAE-conjugated MMOT05530A ADC, DMOT4039A (Genentech/Roche), in patients with pancreatic and ovarian cancers.[48] In a preclinical study preceding the clinical trial, ^{89}Zr-MMOT0530A was used for PET imaging of MSLN-expressing human pancreatic tumor xenografts.[13] A dose escalation study of 10, 25, and 100 μg of ^{89}Zr-MMOT0530A, injected in the presence of an equal dose of an ^{111}In-labeled nonspecific control, showed highest uptake in HPAC tumors in the lowest dose group (14.2 $\pm$ 2.5%ID/g, 11.1 $\pm$ 0.6%ID/g, and 7.5 $\pm$ 1.1%ID/g, respectively). This could likely be attributed to saturation of MSLN binding sites at higher doses. PET data from HPAC and Capan-2 tumor-bearing mice injected with 10 μg of ^{89}Zr-MMOT0530A showed similar tumor uptake that increased over six days, whereas activity in other tissues decreased. Ex vivo biodistribution analyses were consistent with imaging data for both xenograft models. Since the relative expression levels of MSLN in these xenograft cell lines was not shown, it is unclear whether the comparable tumor uptake was a result of similar MSLN expression levels in vivo. However, if MSLN expression in the two xenografts was different, the equivalence in tumor uptake could be due to the injected dose being below the saturation limit or potential differences in MSLN internalization rates. In fact, another related publication did characterize MSLN expression of Capan-1 and HPAC in vitro and in vivo.[49] This study compared tumor uptake of ^{89}Zr-MMOT0530A with the therapeutic efficacy of the DMOT4039A using six different human cancer cell line xenografts that were shown to express different levels of MSLN (OVCAR-3x2.1 ovarian adenocarcinoma; HPAC, Capan-2, HPAF-II, and AsPC-1 pancreatic adenocarcinoma; and MSTO-211H pleural mesothelioma). For the imaging and efficacy studies, mice were injected with 5 mg/kg ($\sim$100 μg) of ^{89}Zr-MMOT0530A or ADC, respectively. Of the six xenografts, only three responded to ADC treatment. Since all cancer cell lines were prescreened for MMAE sensitivity, this finding was attributed to lower MSLN expression levels in the three

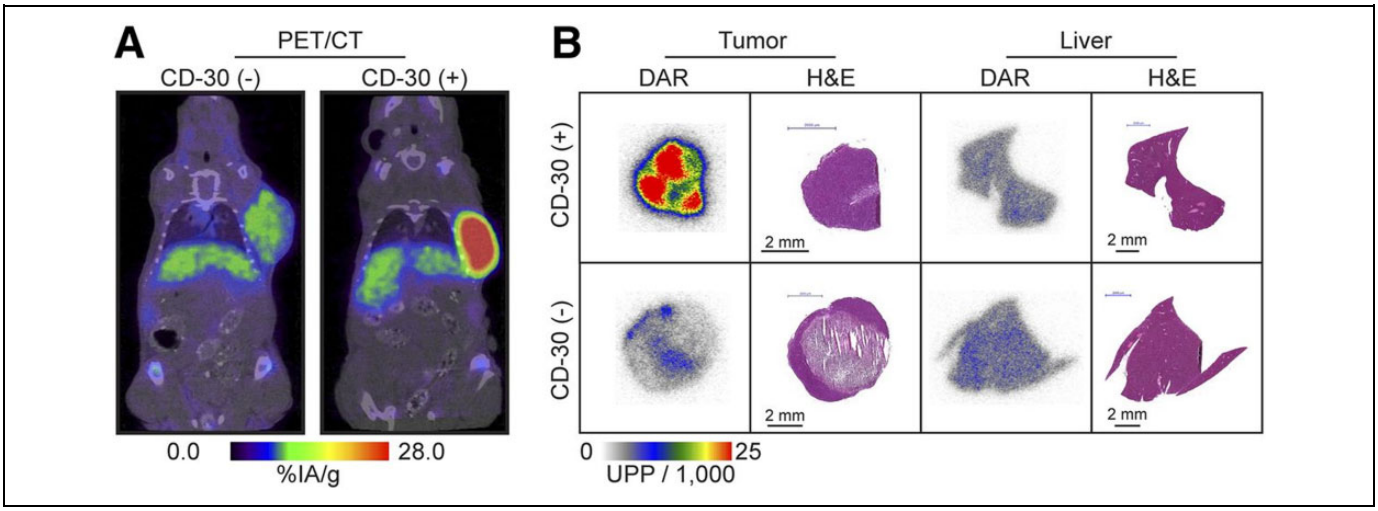

Figure 4. PET/CT images of CD30^{-} and CD30^{+} mice at 144 hours after injection of the ^{89}Zr-labeled mAb (AC-10; A) and the corresponding digital autoradiography (DAR) and hematoxylin and eosin (H&E) staining (B). Adapted from Rylova et al.[47]

nonresponders and/or potential differences in target internalization. OVCAR-3x2.1 xenografts exhibited the most significant response, followed by HPAC, and Capan-2, respectively. Similarly, PET imaging of ^{89}Zr-MMOT0530A six days postinjection demonstrated highest tumor uptake in the same three xenografts, although only 2-fold greater signal than nontargeting control (OVCAR-3x2.1, 10.4%ID/g $\pm$ 0.8%ID/g; Capan-2, 8.8%ID/g $\pm$ 1.0%ID/g; HPAC, 6.0%ID/g $\pm$ 1.2%ID/g). Consistent with the previous study, Capan-2 and HPAC xenografts exhibited similar tumor uptake,[13,49] although MSLN expression in Capan-2 tumors was slightly lower. Overall, the authors concluded that in all cases, the immuno-PET signals predicted ADC-mediated tumor growth inhibition. However, it is important to note that while immuno-PET can act as a surrogate for ADC uptake in tumors, it may be limited in predicting efficacy due to other contributing factors including tumor drug sensitivity, resistance mechanisms, and the extent of target internalization.

TENB2 and STEAP1 in Prostate Cancer

Transmembrane proteoglycan, related to the epidermal growth factor family of growth factors and follistatin (TENB2) and six-transmembrane epithelial antigen of the prostate-1 (STEAP1), were shown to be highly expressed in prostate tumors, and mAbs targeting these two proteins were evaluated by immuno-PET and as ADCs for targeted treatment of prostate cancer.[50] Ex vivo tumor tracer uptake of ^{111}In-labeled TENB2 and STEAP1 mAbs (5 mg/kg) was assessed in four patient-derived xenograft prostate tumor models three days postinjection: LuCaP35V, LuCaP70, LuCaP77, and LuCaP96.1. For TENB2, highest tumor uptake was observed in LuCaP77 (96.1%ID/g $\pm$ 2.8%ID/g) followed by LuCaP96.1, LuCaP70, and LuCaP35V (12.2%ID/g $\pm$ 1.6%ID/g), respectively. For STEAP1, LuCaP35V tumors exhibited the highest uptake (38.7%ID/g $\pm$ 1.5%ID/g) followed by LuCaP77, LuCaP70, and LuCaP96.1 (4.7%ID/g $\pm$ 0.3%ID/g), respectively. Antitumor efficacy with the MMAE-conjugated ADCs was shown to be consistent with the uptake studies. The TENB2-targeted ADC demonstrated greatest efficacy against LuCaP96.1 and LuCaP70, whereas LuCaP77 showed early effects followed by recurrence, suggestive of MMAE resistance. The anti-STEAP1 ADC inhibited growth of LuCaP35V and LuCaP70 tumors, which showed greatest ^{111}In-labeled STEAP1 mAb uptake. Furthermore, ^{89}Zr-immuno-PET was used as a quantitative measure of tracer uptake and correlated with ^{111}In biodistribution studies, and was relatively consistent with immunohistochemistry and FACS analysis of TENB2 and STEAP1 expression. This study provides further evidence that immuno-PET data can be extremely beneficial in predicting ADC binding, internalization, and antitumor efficacy in vivo.

LGR5 in Colon Cancer

LGR5 is highly expressed in approximately 60% to 70% of colorectal adenocarcinomas with low expression in normal tissues.[16] LGR5^{+} colon cancer cells have been shown to function as cancer stem cells that drive tumor growth and metastasis,[51,52]thus making it a promising target for the development of novel therapeutics. Two anti-LGR5 mAbs (8F2 and 9G5) were evaluated using ^{89}Zr-immuno-PET to select the optimal mAb for imaging of LGR5 and ADC development.[53] Both mAbs demonstrated specific, high-affinity binding, and internalization in LGR5-overexpressing 293T (293T-LGR5) and DLD-1 colorectal cancer cells, but not 293T-vector cells or DLD-1 cells with LGR5 shRNA knockdown (DLD-1-shLGR5). ^{89}Zr-DFO-LGR5 mAbs were generated and shown to retain high affinity and LGR5-dependent uptake in vitro. PET imaging of DLD-1 tumor xenografts performed five days postinjection showed higher tumor signal for ^{89}Zr-DFO-8F2

versus ^{89}Zr-DFO-9G5, with tumor-to-muscle ratios of 16.2 ± 2.1 and 8.0 ± 1.0, respectively. Similarly, biodistribution data showed significantly higher tumor uptake for ^{89}Zr-DFO-8F2 (17.9%ID/g ± 2.2%ID/g) compared to ^{89}Zr-DFO-9G5 (5.5%ID/g ± 1.2%ID/g). No significant uptake was observed in DLD-1-shLGR5 tumors or for control ^{89}Zr-DFO-IgG. The anti-LGR5 mAbs were prescreened in vitro for ADC activity by complexing with a duocarmycin-conjugated secondary ADC and testing the ability of the complex to destroy LGR5-expressing colon cancer cells. Although both mAbs induced LGR5-dependent cytotoxicity, 8F2 exhibited slightly higher potency. Taken together, 8F2 was identified as the best candidate for ADC development and confirmed findings from a prior therapeutic study with MMAE-conjugated 8F2, which was shown to eradicate LGR5-positive tumors in vivo and prevent recurrence.[16] Together, these studies demonstrate that ^{89}Zr-labeled anti-LGR5 mAbs can identify tumors with high LGR5 expression and that immuno-PET may be used as a tool to improve mAb selection for the development of LGR5-targeted ADCs. Furthermore, LGR5 imaging may be useful for stratifying patients who would respond best to an LGR5-targeted ADC therapy and for monitoring treatment response.

Clinical Uses of Immuno-PET With ADCs

The ZEPHIR Trial for Breast Cancer

The recent FDA approval of T-DM1 provided a new therapeutic option for patients with HER2$^+$ breast cancer who progressed following prior treatment with trastuzumab. For this agent, HER2 overexpression enables receptor-mediated delivery of DM1, a highly potent analog of the microtubule inhibitor maitansine. Given the need for confirming HER2$^-$ positivity as a prerequisite for therapy and the established difficulties with tissue biopsies, the use of molecular imaging for patient selection was proposed by Gebhart and colleagues in the ZEPHIR trial and represents the first prospective and comprehensive imaging study in advanced HER2$^+$ breast cancer.[54] The goal of the study was to determine eligibility for receiving T-DM1 and consisted of 60 patients with progressive HER2$^+$ breast cancer. Patients underwent ^{89}Zr-trastuzumab imaging before and after three cycles of T-DM1 therapy, as well as ^{18}F-fluorodeoxyglucose (FDG) PET imaging as an indicator of early metabolic response to complement immuno-PET findings. Significant heterogeneity in ^{89}Zr-trastuzumab scans was observed and resulted in patients being categorized into four groups, representing different tracer uptake patterns (Figure 5). From the 39 patients who were classified as HER2$^+$ by immuno-PET, 28 showed objective response on computed tomography (CT) after T-DM1 therapy to give a positive predictive value (PPV) of 72%. In cases where patients were classified as HER2$^-$ and stable or progressive disease was shown by CT, a negative predictive value (NPV) of 88% (14 of 16) was determined. Metabolic imaging with FDG provided a PPV of 96% and an NPV of 83%, and the combination of both molecular imaging approaches gave a PPV and NPV of 100% based on response evaluation criteria in solid tumors.

Selecting the appropriate outcome is key in evaluating the effectiveness of molecular imaging agents. Median time-to-treatment failure (TTF) was selected in this study, since it represents the time point when the benefit of continuing therapy is no longer evident. By evaluating the correlation between molecular imaging and TTF, physicians will have a better understanding of how a patient may respond to ADC therapy and change the course of treatment where needed without subjecting patients to unnecessary periods of ineffective therapy. Patients in the positive immuno-PET imaging group had a median TTF of 11.2 months compared to 3.5 months for those with negative immuno-PET scans. Combining immuno-PET and metabolic imaging further distinguished this difference, resulting in a median TTF of 15 months for patients with positive HER2 and FDG scans when compared to 2.8 months in patients with negative findings from both scans. Patients with low (or no) ^{89}Zr-trastuzumab uptake in metastatic lesions also had shorter median TTF than those with homogenous tracer uptake, further demonstrating the potential role of immuno-PET as a predictor of patient response. This study elegantly displayed the potential of molecular imaging as a companion diagnostic for ADC therapy by focusing on patient individualization via immuno-PET and combinatorial imaging strategies that incorporated metabolic imaging. Methodology from the ZEPHIR trial could be expanded to other ADCs to (1) improve the understanding of how effective these new therapies may be and (2) validate the role of molecular imaging as a biomarker that can be broadly applied in drug development studies.

MSLN-Targeted Imaging and Therapy

Lamberts et al used ^{89}Zr-immuno-PET to determine how tracer antibody uptake relates to MSLN target expression and therapeutic response to the ADC, DMOT4039A, in patients with pancreatic and ovarian cancer.[48] Prior to ADC administration, a total of 11 patients received ^{89}Zr-MMOT0530A with mean radioactivity of 37 MBq followed by imaging at 2, 4, and 7 days postinjection. Two patients were administered 1 mg of ^{89}Zr-MMOT0530A and the remaining nine received a total of 10 mg labeled and unlabeled antibody. The latter was determined to be the suitable dose due to the increase in tracer antibody availability in circulation. Maximum tumor uptake was detected four days post injection in 17 pancreatic and 20 ovarian cancer lesions, with a SUV_{max} of 11.5 ± 7.5 and 14.5 ± 8.7, respectively. The authors suggested that lower uptake observed in pancreatic tumors may be attributed to the presence of dense stromal tissue making the environment inaccessible to antibody. Another possibility is that there is overall lower expression of target antigen at the tumor surface in pancreatic versus ovarian tumors. Uptake (reported as %ID/g) in blood (7.9 ± 2.2), liver (13.2 ± 4.1), kidneys (9.1 ± 4.5), spleen (8.0 ± 2.7), and intestine (8.0 ± 2.7) all reflected normal antibody distribution. Heterogeneity of ^{89}Zr-MMOT0530A tumor uptake occurred both intrapatient,

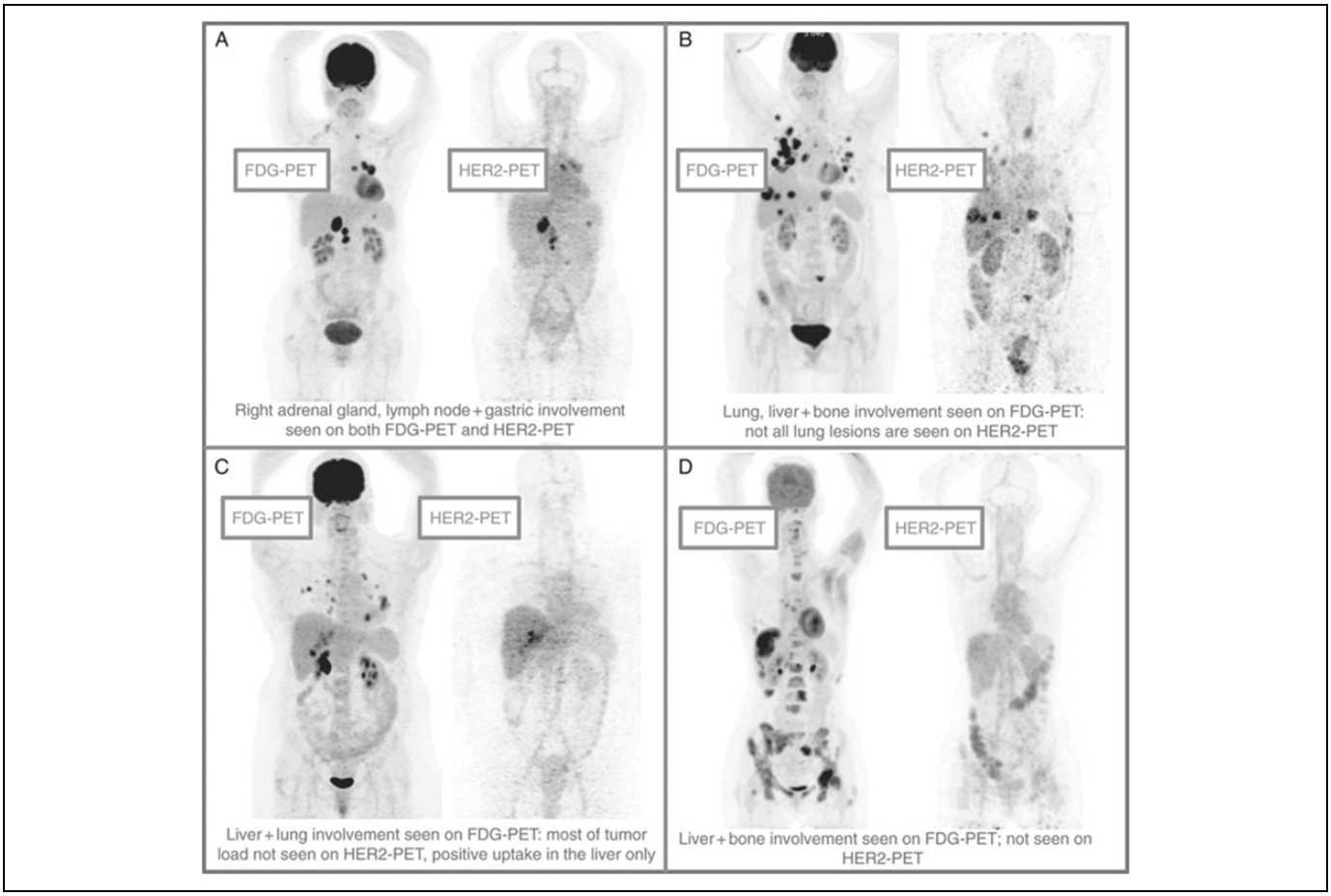

Figure 5. Patterns of HER2–PET/CT confronted with FDG–PET/CT, maximum intensity projection. Lesion uptake was considered pertinent when visually higher than blood pool. (A) Entire tumor load showed pertinent tracer uptake; (B) dominant part of tumor load showed tracer uptake; (C) minor part of tumor load showed tracer uptake; and (D) entire tumor load lacked tracer uptake (adapted from Gebhart et al[54]).

with a 2.4-fold mean tumor uptake difference, and between patients, with mean difference of 5.3-fold. The MSLN expression determined by immunohistochemistry (IHC) did not correlate with PET uptake in this study. This result may be due to the use of archival tumor sections which may represent only a fraction of the entire tumor, whereas PET provides assessment of the entire tumor. The authors suggest that fresh tumor biopsies would provide a more accurate comparison. Additionally, the use of two different antibodies may also contribute to the observed discrepancy between approaches, since antibodies can differ in epitope binding and affinity. In 9 of 11 patients treated with DMOT4039A, the best response was stable disease, while 1 patient experienced immediate progressive disease and 1 had a confirmed partial response. Although PET uptake did not correlate with progression-free survival on a per-patient basis, the patient with ongoing partial response showed PET tracer uptake in two liver metastases and in the primary pancreatic tumor. Although the clinical evaluation for DMOT4039A was later halted,[8] these studies demonstrated that immuno-PET imaging of tumor antigens such as MSLN can provide useful information for the selection of patients that are most likely to benefit from target-based therapy.

Perspective and Future Directions

There are multiple motivating factors for the use of ^{89}Zr-immuno-PET imaging in both the preclinical and the clinical development of ADCs. In addition to confirming target-specific tumor localization and uptake, imaging can be utilized to assess the pharmacokinetics of ADCs and would aid in understanding how blood residence times impact target and off-target effects. This is particularly important because of the inherently long circulation time of mAbs in blood, which while providing drug exposure to tumors, could also increase systemic toxicity. Lamberts et al were the first to utilize ^{89}Zr-immuno-PET imaging as a biomarker for whole-body imaging to determine potential tissue toxicity and verify targeted delivery of an anti-MSLN antibody at the tumor site.[48] Ultimately, in their study, imaging would serve as a means to predict response to therapy. However, the authors did not observe a correlation between PET uptake and progression-free survival. The assumption was made that successful tumor uptake of radiolabeled antibody would result in increased ADC efficacy, which is not always the case since drug conjugation can significantly alter the pharmacokinetics and stability of the

unconjugated antibody.[55] Jacobson et al observed this by examining the impact of drug conjugation on the in vivo properties of radiolabeled mAbs and ADCs, and found that ADCs had higher lipophilic character than their nonpayload containing counterparts.[56] They also showed lower blood half-life for the ADCs, indicating faster clearance following attachment of the payload. Importantly, their analysis revealed a 50-60 reduction in tumor uptake following drug conjugation, suggesting that use of the naked mAbs as a companion diagnostic would have overestimated ADC uptake in tumors and provided an inaccurate prediction of drug delivery. Thus, ^{89}Zr-labeling and imaging of the ADCs themselves may be more beneficial at predicting therapeutic efficacy, dosing, and potential normal tissue toxicity. In fact, the ZEPHIR trial proved to more accurately predict response to therapy, since it combined ^{89}Zr-trastuzumab PET/CT and FDG imaging with an early response assessment to T-DM1 in patients with HER2^{+} breast cancer.[54] This multimodal approach provided a better understanding of how individual patients would respond to the ADC without subjecting them to ineffective treatment and toxicity, while also eliminating unnecessary drug costs.

Presently, IHC is a major analytical tool used for target evaluation and patient selection for targeted therapies, including ADCs. However, in the anti-MSLN antibody study, immuno-PET uptake did not correlate with MSLN expression determined by IHC.[48] The downside of IHC is that it requires an invasive procedure and is often performed upon an archival formalin-fixed paraffin embedded (FFPE) tumor section of a single lesion that fails to represent the heterogeneity of the entire tumor or multiple lesions. The IHC procedures can also be easily compromised due to sampling errors or artifacts. Furthermore, therapeutic antibodies that bind native receptor may fail to bind and detect receptor levels in FFPE tissues as a result of target inaccessibility or destruction of antigen. Conversely, ^{89}Zr-immuno-PET provides an assessment of target levels, accessibility, and accumulation for all tumor lesions and normal tissues non-invasively. Thus, imaging can be a valuable adjunct to IHC and serve as a functional tool to confirm that an ADC hits its target throughout the body. With further optimization and standardization, ^{89}Zr-immuno-PET has great potential to function as a predictive biomarker of an ADC effectiveness. The knowledge acquired from immuno-PET coupled with preclinical findings could be employed to determine optimal and individualized dosing regimens for patients in order to maximize the therapeutic effect and safety of novel ADC therapies.

Declaration of Conflicting Interests

The author(s) declared no potential conflicts of interest with respect to the research, authorship, and/or publication of this article.

Funding

The author(s) disclosed receipt of the following financial support for the research, authorship, and/or publication of this article: This work was supported by the John S. Dunn Research Scholar Fund (A. Azhdarinia) and Welch Foundation Endowment Fund (Welch award L-AU-0002-19940421; K.S. Carmon).

References

1. Panowski SS, Bhakta H, Raab P, et al. Site-specific antibody drug conjugates for cancer therapy. In: *MAbs*. Vol. 6. No. 1. Taylor & Francis; 2014:34–45.
2. Teicher BA. Antibody–drug conjugate targets. *Curr Cancer Drug Targets*. 2009;9(8):982–1004.
3. Trail PA. Antibody drug conjugates as cancer therapeutics. *Antibodies*. 2013;9:113–129.
4. Niculescu-Duvaz I. Technology evaluation: gemtuzumab ozogamicin, celltech group. *Curr Opin Mol Ther*. 2000;2(6):691–696.
5. Senter PD, Sievers EL. The discovery and development of brentuximab vedotin for use in relapsed Hodgkin lymphoma and systemic anaplastic large cell lymphoma. *Nat Biotechnol*. 2012; 30(7):631–637.
6. Lambert JM, Chari RV. Ado-trastuzumab emtansine (T-DM1): an antibody–drug conjugate (ADC) for HER2-positive breast cancer. *J Med Chem*. 2014;57(16):6949–6964.
7. DiJoseph JF, Dougher MM, Kalyandrug LB, et al. Antitumor efficacy of a combination of CMC-544 (inotuzumab ozogamicin), a CD22-targeted cytotoxic immunoconjugate of calicheamicin, and rituximab against non-Hodgkin's B-cell lymphoma. *Clin Cancer Res*. 2006;12(1):242–249.
8. Beck A, Goetsch L, Dumontet C, Corvaia N. Strategies and challenges for the next generation of antibody–drug conjugates. *Nat Rev Drug Discov*. 2017;16(5):315–337.
9. Mullard A. Maturing antibody–drug conjugate pipeline hits 30. *Nat Rev Drug Discov*. 2013;12(5):329–332.
10. Sharkey RM, Govindan SV, Cardillo TM, et al.Selective and concentrated accretion of SN-38 with a CEACAM5-targeting antibody-drug conjugate (ADC), labetuzumab govitecan (IMMU-130). *Mol Cancer Ther*. 2017;17(1):196–203.
11. Rudin CM, Pietanza MC, Bauer TM, et al.Rovalpituzumab tesirine, a DLL3-targeted antibody–drug conjugate, in recurrent small-cell lung cancer: a first-in-human, first-in-class, open-label, phase 1 study. *Lancet Oncol*. 2017;18(1):42–51.
12. Saunders LR, Bankovich AJ, Anderson WC, et al.A DLL3-targeted antibody–drug conjugate eradicates high-grade pulmonary neuroendocrine tumor-initiating cells in vivo. *Sci Transl Med*. 2015;7(302):302ra136.
13. ter Weele EJ, Terwisscha van Scheltinga AG, Kosterink JG, et al. Imaging the distribution of an antibody–drug conjugate constituent targeting mesothelin with (8)(9)Zr and IRDye 800CW in mice bearing human pancreatic tumor xenografts. *Oncotarget*. 2015; 6(39):42081–42090.
14. Pereira DS, Guevara CI, Jin L, et al. AGS67E, an anti-CD37 monomethyl auristatin E antibody–drug conjugate as a potential therapeutic for B/T-cell malignancies and AML: a new role for CD37 in AML. *Mol Cancer Ther*. 2015;14(7):1650–1660.
15. Visintin A, Knowlton K, Tyminski E, et al. Novel anti-TM4SF1 antibody–drug conjugates with activity against tumor cells and tumor vasculature. *Mol Cancer Ther*. 2015;14(8):1868–1876.

16. Gong X, Azhdarinia A, Ghosh SC, et al. LGR5-targeted antibody–drug conjugate eradicates gastrointestinal tumors and prevents recurrence. *Mol Cancer Ther*. 2016;15(7):1580–1590.
17. Junttila MR, Mao W, Wang X, et al. Targeting LGR5+ cells with an antibody–drug conjugate for the treatment of colon cancer. *Sci Transl Med*. 2015;7(314):314ra186.
18. Lehar SM, Pillow T, Xu M, et al. Novel antibody-antibiotic conjugate eliminates intracellular *S. aureus*. *Nature*. 2015;527(7578): 323–328.
19. Wang RE, Liu T, Wang Y, et al. An immunosuppressive antibody–drug conjugate. *J Am Chem Soc*. 2015;137(9):3229–3232.
20. Senter PD. Potent antibody drug conjugates for cancer therapy. *Curr Opin Chem Biol*. 2009;13(3):235–244.
21. Tolcher AW, Sugarman S, Gelmon KA, et al. Randomized phase II study of BR96-doxorubicin conjugate in patients with metastatic breast cancer. *J Clin Oncol*. 1999;17(2):478–484.
22. Smith LM, Nesterova A, Alley SC, Torgov MY, Carter PJ. Potent cytotoxicity of an auristatin-containing antibody–drug conjugate targeting melanoma cells expressing melanotransferrin/p97. *Mol Cancer Ther*. 2006;5(6):1474–1482.
23. Sutherland MK, Yu C, Lewis TS, et al. Anti-leukemic activity of lintuzumab (SGN-33) in preclinical models of acute myeloid leukemia. *MAbs*. 2009;1(5):481–490.
24. Wang X, Ma D, Olson WC, Heston WD. In vitro and in vivo responses of advanced prostate tumors to PSMA ADC, an auristatin-conjugated antibody to prostate-specific membrane antigen. *Mol Cancer Ther*. 2011;10(9):1728–1739.
25. Asundi J, Reed C, Arca J, et al. An antibody–drug conjugate targeting the endothelin B receptor for the treatment of melanoma. *Clin Cancer Res*. 2011;17(5):965–975.
26. Dokter W, Ubink R, van der Lee M, et al. Preclinical profile of the HER2-targeting ADC SYD983/SYD985: introduction of a new duocarmycin-based linker-drug platform. *Mol Cancer Ther*. 2014;13(11):2618–2629.
27. McKnight BN, Viola-Villegas NT. (89) Zr-ImmunoPET companion diagnostics and their impact in clinical drug development. *J Labelled Comp Radiopharm*. 2018;61(9):727–738.
28. van Dongen GA, Visser GW, Lub-de Hooge MN, de Vries EG, Perk LR. Immuno-PET: a navigator in monoclonal antibody development and applications. *Oncologist*. 2007;12(12): 1379–1389.
29. van Dongen GA, Vosjan MJ. Immuno-positron emission tomography: shedding light on clinical antibody therapy. *Cancer Biother Radiopharm*. 2010;25(4):375–385.
30. Van Dongen GA, Huisman MC, Boellaard R, et al. ^{89}Zr-immuno-PET for imaging of long circulating drugs and disease targets: why, how and when to be applied? *Q J Nucl Med Mol Imaging*. 2015;59(1):18–38.
31. Cohen R, Vugts DJ, Visser GW, et al. Development of novel ADCs: conjugation of tubulysin analogues to trastuzumab monitored by dual radiolabeling. *Cancer Res*. 2014;74(20):5700–5710.
32. Sijbrandi NJ, Merkul E, Muns JA, et al. A novel platinum(II)-based bifunctional ADC linker benchmarked using 89Zr-desferal and auristatin F-conjugated trastuzumab. *Cancer Res*. 2017;77(2): 257–267.
33. Muns JA, Montserrat V, Houthoff HJ, et al. In vivo characterization of platinum(II)-based linker technology for the development of antibody–drug conjugates: taking advantage of dual labeling with (195 m)Pt and (89)Zr. *J Nucl Med*. 2018;59(7):1146–1151.
34. Wright BD, Lapi SE. Designing the magic bullet? The advancement of immuno-PET into clinical use. *J Nucl Med*.2013;54(8): 1171–1174.
35. Heskamp S, Raave R, Boerman O, Rijpkema M, Goncalves V, Denat F. (89)Zr-immuno-positron emission tomography in oncology: state-of-the-art (89)Zr radiochemistry. *Bioconjug Chem*. 2017;28(9):2211–2223.
36. Niccoli Asabella A, Cascini GL, Altini C, Paparella D, Notaristefano A, Rubini G. The copper radioisotopes: a systematic review with special interest to 64Cu. *Biomed Res Int*. 2014; 2014:786463.
37. Nayak TK, Brechbiel MW. 86Y based PET radiopharmaceuticals: radiochemistry and biological applications. *Med Chem*. 2011; 7(5):380–388.
38. Jauw YW, Menke-van derHouven van Oordt CW, Hoekstra OS, et al. Immuno-positron emission tomography with zirconium-89-labeled monoclonal antibodies in oncology: what can we learn from initial clinical trials? *Front Pharmacol*. 2016;7:131.
39. Deri MA, Zeglis BM, Francesconi LC, Lewis JS. PET imaging with 89Zr: from radiochemistry to the clinic. *Nucl Med Biol*.2013; 40(1):3–14.
40. Holland JP, Divilov V, Bander NH, Smith-Jones PM, Larson SM, Lewis JS. 89Zr-DFO-J591 for immunoPET of prostate-specific membrane antigen expression in vivo. *J Nucl Med*. 2010;51(8): 1293–1300.
41. Abou DS, Ku T, Smith-Jones PM. In vivo biodistribution and accumulation of ^{89}Zr in mice. *Nucl Med Biol*. 2011;38(5): 675–681.
42. Holland JP, Sheh Y, Lewis JS. Standardized methods for the production of high specific-activity zirconium-89. *Nucl Med Biol*. 2009;36(7):729–739.
43. Vosjan MJ, Perk LR, Visser GW, et al. Conjugation and radiolabeling of monoclonal antibodies with zirconium-89 for PET imaging using the bifunctional chelate p-isothiocyanatobenzyl-desferrioxamine. *Nat Protoc*. 2010;5(4):739–743.
44. Verel I, Visser GW, Boellaard R, Stigter-van Walsum M, Snow GB, van Dongen GA. 89Zr immuno-PET: comprehensive procedures for the production of 89Zr-labeled monoclonal antibodies. *J Nucl Med*. 2003;44(8):1271–1281.
45. van der Weyden CA, Pileri SA, Feldman AL, Whisstock J, Prince HM. Understanding CD30 biology and therapeutic targeting: a historical perspective providing insight into future directions. *Blood Cancer J*. 2017;7(9):e603.
46. Yi JH, Kim SJ, Kim WS. Brentuximab vedotin: clinical updates and practical guidance. *Blood Res*. 2017;52(4):243–253.
47. Rylova SN, Del Pozzo L, Klingeberg C, et al. Immuno-PET imaging of CD30-positive lymphoma using ^{89}Zr-desferrioxamine-labeled CD30-specific AC-10 antibody. *J Nucl Med*. 2016;57(1):96–102.
48. Lamberts LE, Menke-van derHouven van Oordt CW, ter Weele EJ, et al. ImmunoPET with anti-mesothelin antibody in patients with pancreatic and ovarian cancer before anti-mesothelin

antibody–drug conjugate treatment. *Clin Cancer Res*. 2016;22(7): 1642–1652.
49. Terwisscha van Scheltinga AG, Ogasawara A, Pacheco G, et al. Preclinical efficacy of an antibody–drug conjugate targeting mesothelin correlates with quantitative 89Zr-immunopet. *Mol Cancer Ther*. 2017;16(1):134–142.
50. Williams SP, Ogasawara A, Tinianow JN, et al. ImmunoPET helps predicting the efficacy of antibody–drug conjugates targeting TENB2 and STEAP1. *Oncotarget*. 2016;7(18):25103–25112.
51. Melo FS, Kurtova AV, Harnoss JM, et al. A distinct role for Lgr5+ stem cells in primary and metastatic colon cancer. *Nature*. 2017;543(7647):676–680.
52. Shimokawa M, Ohta Y, Nishikori S, et al. Visualization and targeting of LGR5+ human colon cancer stem cells. *Nature*. 2017; 545(7653):187–192.
53. Azhdarinia A, Voss J, Ghosh SC, et al. Evaluation of anti-LGR5 antibodies by immunoPET for imaging colorectal tumors and development of antibody–drug conjugates. *Mol Pharm*. 2018; 15(6):2448–2454.
54. Gebhart G, Lamberts LE, Wimana Z, et al. Molecular imaging as a tool to investigate heterogeneity of advanced HER2-positive breast cancer and to predict patient outcome under trastuzumab emtansine (T-DM1): the ZEPHIR trial. *Ann Oncol*. 2016;27(4):619–624.
55. Perez HL, Cardarelli PM, Deshpande S, et al. Antibody-drug conjugates: current status and future directions. *Drug Discov Today*. 2014;19(7):869–881.
56. Jacobson O, Li Q, Chen H, et al. PET-guided evaluation and optimization of internalized antibody–drug conjugates targeting erythropoietin-producing hepatoma A2 receptor. *J Nucl Med*. 2017;58(11):1838–1844.